ONE-STEP INJECTABLE AND BIOREDUCIBLE POLY(β-AMINO ESTER) HYDROGELS AS CONTROLLED DRUG DELIVERY PLATFORMS

Betul Bingol [†], Seckin Altuncu[†], Fatma Demir Duman [‡], Ayse Ak[‡§], Umit Gulyuz[⊥∥], Havva Yagci Acar[‡], Oguz Okay[⊥], Duygu Avci[†]*

[†]Department of Chemistry, Bogazici University, 34342, Bebek, Istanbul, Turkey

[‡]Department of Chemistry, Koc University, 34450, Sariyer, Istanbul, Turkey

[⊥]Department of Chemistry, Istanbul Technical University, Maslak, 34469 Istanbul, Turkey

[∥]Department of Chemistry and Chemical Processing Technologies, Kirklareli University, Luleburgaz 39750, Kirklareli, Turkey

KEYWORDS

Hydrogel, Biodegradable polymers, Poly(β-amino ester)s, Controlled release, Photodynamic therapy.

ABSTRACT

A one-step synthesis strategy based on aza-Michael reaction of poly(ethylene glycol) diacrylate (PEGDA) or PEGDA/1,6-hexanediol diacrylate (HDDA) mixture and cystamine was employed to fabricate injectable, biocompatible and degradable novel poly(β-amino ester) (PBAE) hydrogels. The gelation was monitored by real-time dynamic rheological measurements in order to follow formation of the PBAE hydrogel networks. The obtained hydrogels were responsive to both pH and redox state which enabled the control of swelling, degradation and release properties by external triggers. Degradation products of the hydrogels were shown to have no significant cytotoxicity on A549 adenocarcinomic human alveolar basal epithelial cells and MCF-7 human breast cancer cells. The hydrogels were loaded with a photosensitizer, methylene blue (MB), as a model compound by simply adding the MB molecules into the precursor mixture. The activity of released MB was assessed by *in vitro* photodynamic therapy (PDT) studies conducted with A549 cells.

INTRODUCTION

Hydrogels are three dimensional hydrophilic polymer networks capable of absorbing high amounts of water [1]. The high water content and permeable pores allowing diffusion of essential nutrients make hydrogel structure similar to that of soft tissues in the body. Therefore, hydrogels have been widely exploited for biomedical applications such as tissue engineering and delivery of therapeutic agents [2-3]. Poly(β-amino ester)s (PBAEs) are biodegradable and biocompatible polymers which are synthesized by step-growth polymerization via aza-Michael reaction of diamines and diacrylates [4]. In many studies PBAEs have been proven to give successful results as potential biomaterials for tissue engineering scaffolds, non-viral vectors for gene delivery, and

depots for sustained release of drugs [5-13]. Biomedical applications of PBAEs have been reported in a detailed review by Liu et. al. [14].

PBAE based biodegradable 3D networks can be easily prepared by a one-step "A2 + B4" Michael addition strategy reported by Biswal et al. [15]. Hyperbranched PBAEs with fluorescent properties, superelastic PBAE cryogels and PBAE networks with inherent antioxidant property have been synthesized by the aforementioned one-step method [16-18]. The diacrylate and tetrafunctional diamine mixture can be directly injected to target site with minimal surgical invasion where it gels in situ under physiological conditions [19-20]. Recently, Xu et. al. reported an injectable hyperbranched PBAE/hyaluronic acid hydrogel with on-demand degradation properties for wound healing and a poly(β-hydrazide ester)/hyaluronic acid hydrogel with antioxidative properties by the one-step method [21-22]. The use of injectable one-step synthesis approach is particularly advantageous for the construction of controlled drug release systems since the therapeutic cargo molecules can be encapsulated in the hydrogel network by simply adding them into the precursor mixture. Furthermore, this method provides mild encapsulation conditions for cargo molecules, especially for sensitive biomolecules in order to retain their biological activity.

The degradation rate, and hence the mechanical properties of PBAE hydrogels can be tailored through selection of building blocks and design of chemical structure. Recently, incorporation of responsive domains into PBAE networks has been reported to trigger the degradation and release upon changes in pH, UV light, or redox state [23-26]. Among these triggers redox state is especially convenient for biomedical applications. For example, the disulfide bond is stable against hydrolysis in the body but is prone to selective cleavage in the reducing environment of tumor tissue and intracellular compartments through thiol–disulfide exchange reactions [27]. Hence, the

disulfide bond is widely utilized via incorporation into polymeric drug delivery systems or hydrogels to control the redox-dependent degradation and release kinetics [28].

Photodynamic therapy (PDT) is an effective clinical treatment modality against various cancer types and infections [29]. Its mechanism of action involves activation of a photosensitizer molecule with a light source of appropriate wavelength [30]. Irradiation of the photosensitizer triggers photochemical reactions which generate cytotoxic reactive oxygen species, particularly singlet oxygen, and induce damage to target cells [31]. Application of PDT locally at the target site is very attractive, both to reduce systematic toxicity and to achieve highly effective results. But localizing the photosensitizer at the target site is difficult due to the small molecular nature of most photosensitizers. Some sensitizers also lack sufficient water solubility or stability. From this perspective, hydrogels which remain at the target site due to their low fluidity, are valuable carriers for photosensitizers to enable topical PDT with spatial and temporal control [32]. Hence, many hydrogel-based drug delivery systems for encapsulation of photosensitizers have been designed and explored for their potential use in photodynamic therapy [33-41].

This study describes fabrication of pH and redox responsive PBAE hydrogels as platforms for controlled drug release. The hydrogels were fabricated by aza-Michael reaction between cystamine and diacrylates, namely poly(ethylene glycol) diacrylate (PEGDA) and 1,6-hexanediol diacrylate (HDDA) by a facile one-step strategy. In the literature, one-step reactions were performed in bulk or in solvents such as DMSO or DMF; at high temperatures and for longer periods of time [14, 16, 18]. In our synthesis method, we used water as the solvent to accelerate hydrogel formation and decrease reaction time to less than 1 h. The therapeutic cargo molecules can be encapsulated in the hydrogel network by simply adding them into the precursor mixture under these mild conditions which is significant for sensitive biomolecules in order to retain their biological activity.

Besides, the incorporation of the hydrophobic monomer HDDA enables tunable hydrolysis rate, giving degradation times of 1 to more than 10 days for the hydrogels. Real-time dynamic rheological measurements were used in order to probe the formation of the PBAE hydrogel networks. Methylene blue (MB), widely used as an inexpensive and non-toxic photosensitizer for PDT, was selected as a model drug to demonstrate the effect of the hydrophobicity of the network on the release kinetics and evaluate the utility of these hydrogels in local PDT [42-44]. To the best of our knowledge, there is only one report about the usage of PBAE-based micelles encapsulated with protoporphyrin for PDT [45]. The toxicity of hydrogel degradation products was evaluated on MCF-7 human breast cancer cells and A549 adenocarcinomic human alveolar basal epithelial cells. *In vitro* PDT potential of released MB was evaluated on A549 cells.

EXPERIMENTAL SECTION

Materials

Cystamine dihydrochloride salt, PEGDA (M_n=575 g/mol), HDDA, 1,4-dithiothreitol (DTT), MB, dimethyl sulfoxide Hybri-Max™ and all solvents were purchased from Sigma-Aldrich (St Louis, MO, USA) and used as received. Penicillin-streptomycin and trypsin-EDTA solutions were provided by Multicell, Wisent Inc. (St. Bruno, QC, Canada). Fetal bovine serum (FBS) was obtained from Capricorn Scientific GmbH (Ebsdorfergrund, Germany). Dulbecco's Modified Eagle Medium (DMEM), phosphate buffer saline (PBS) tablets and thiazolyl blue tetrazolium bromide (MTT) were purchased from Biomatik Corp. (Cambridge, ON, Canada). 96-well plates were obtained from Nest Biotechnology Co. Ltd. (Wuxi, China). MCF-7 human breast cancer cells were given as a gift from Dr. Engin Ulukaya (Department of Medicinal Biochemistry, Faculty of

Medicine, University of Istinye, Istanbul, Turkey). A549 was provided by Prof. Devrim Gozuacik (Sabanci University, Istanbul, Turkey).

Characterization

Thermal analyses were performed with differential scanning calorimetry (DSC) (TA Instruments Q100) under nitrogen atmosphere from -75 °C to 75 °C with a scanning rate of 10 °C/min. The lyophilized hydrogel samples were sputter coated with a platinum layer and their internal fracture surface was examined with scanning electron microscopy (SEM) (FEI-Philips XL30) with an accelerating voltage of 7.0 kV. Degradation and release studies were done using incubator shaker (VWR) operating at 37 °C and 200 rpm. Raman spectra were obtained using Renishaw InVia Raman Microscope. UV-visible spectra were recorded by Shimadzu UV-1201 spectrophotometer.

One-step Synthesis of PBAE Hydrogels

Cystamine was prepared by neutralization of cystamine dihydrochloride with potassium hydroxide according to a procedure described elsewhere [46]. Briefly, a mixture of cystamine dihydrochloride (2 g, 8.88 mmol), potassium hydroxide (1.1 g, 19.54 mmol), and 20 mL methanol was stirred at room temperature for 24 h. The white precipitate was filtered off and the crude product was obtained by evaporating methanol under reduced pressure. The residue was then dissolved in dichloromethane (50 mL), washed with saturated $NaHCO_3$ solution (10 mL) and dried over sodium sulfate. Pure cystamine was obtained with 68% yield after evaporation of dichloromethane. To prepare the one-step PBAE hydrogels, cystamine (0.13 mmol, 20 mg) was dissolved in 0.12-0.2 mL distilled water in a vial and a diacrylate (for H1: 0.26 mmol, 150 mg PEGDA, for H2: 0.13 mmol, 75 mg PEGDA and 0.13 mmol, 30 mg HDDA, for H3: 0.065 mmol,

38 mg PEGDA and 0.195 mmol, 45 mg HDDA) was added. The mixture was placed in an orbital shaker at 37 °C and 200 rpm for 1 hour. The obtained hydrogel samples were dried and weighed to obtain (W_1). Then the hydrogels were immersed in ethanol (20 mL) for 24 h to remove unreacted starting materials. The swollen samples were dried and weighed again to obtain (W_2). The gelation percentage of hydrogel samples, that is, the weight percent of the reactants incorporated into the ethanol-insoluble 3D hydrogel network was calculated by

$$Gelation\ (\%) = \frac{W_2}{W_1} \times 100 \quad (1)$$

One-step Synthesis of drug loaded PBAE Hydrogels

The MB loaded hydrogel samples were fabricated as described for unloaded ones, except that 1 wt % MB (with respect to total hydrogel weight) was dissolved in water and the aqueous MB solution was added to the hydrogel precursor mixture instead of water. The dye loaded hydrogels were immersed in ethanol (20 mL) to get rid of unreacted starting materials and excess dye before release studies. The loading capacity (LC %) was calculated using weights of entrapped drug (W_d) and hydrogel (W_h) by

$$LC\ (\%) = \frac{W_d}{W_h} \times 100 \quad (2)$$

Rheological Experiments

Cystamine (1 mol equiv.) and diacrylate (2 mol equiv.) were dissolved in distilled water in a vial and stirred for a few seconds. The solution was then transferred between the plates of the rheometer (Gemini 150 Rheometer system, Bohlin Instruments) equipped with a cone-and-plate geometry

(cone angle = 4°, diameter = 40 mm) to monitor the reaction by oscillatory small-strain shear measurements at 37 °C. The instrument was equipped with a Peltier device for temperature control. During the rheological measurements, a solvent trap was used and the outside of the upper plate was covered with a thin layer of low-viscosity silicone oil to prevent the evaporation of water. An angular frequency ω of 6.3 rad/s and a deformation amplitude γ_o of 0.01 were selected to ensure that the oscillatory deformation is within the linear regime (Figure S1). Frequency sweep tests were carried out at 37 °C and γ_o = 0.01 over the frequency range 0.06 – 300 rad/s.

Swelling Studies

Swelling studies were performed by immersing dry hydrogel samples into PBS solutions (pH 5 or pH 7.4) at 37 °C. The samples were removed from the solutions, blotted on filter paper, and their swollen weights were measured at different time intervals. The degree of swelling (D_s) was calculated using

$$D_s = \frac{W_s - W_d}{W_d} \times 100 \quad (3)$$

where W_s and W_d refer to the weight of swollen and dry gel samples, respectively. The average values from triplicate measurements were reported.

Degradation of Hydrogels

Hydrogel samples were weighed (W_i) and immersed in 4 mL degradation solution (phosphate buffer solutions of pH 5 and pH 7.4, or 25 mM DTT) at 37 °C. The solution was then placed on an orbital shaker operating at 200 rpm. At predetermined time intervals, the samples were removed from the degradation solution, lyophilized and weighed (W_f). The degradation % was calculated according to

$$Degradation\ (\%) = \frac{W_i - W_f}{W_i} \times 100 \quad (4)$$

In Vitro Release Studies

MB was selected as a model drug to demonstrate the release kinetics of PBAE hydrogels. MB loaded hydrogels were placed in 50 mL phosphate buffer solutions (pH 7.4 and pH 5) and were shaken at 200 rpm using an orbital shaker at 37 °C. At predetermined time intervals, 2 mL of buffer solution was removed and analyzed by UV−visible spectroscopy. The removed aliquots were replaced by fresh buffer solution to maintain the volume of the release medium. The increase in absorbance of the buffer solutions was monitored and the cumulative release of MB was determined using a calibration curve based on the absorbance of MB solutions of known concentrations at 666 nm.

Determination of *in vitro* Cytotoxicity and PDT Studies

For the cytotoxicity evaluation of the degradation products of the gels and for PDT studies, A549 cells were incubated with different concentrations of the degradation products (after 6 h of degradation at pH 7.4 PBS). After culturing of the cells in DMEM complete medium supplemented with 10% (v/v) FBS and 1% (v/v) penicillin-streptomycin in an incubator under 5% CO_2 atmosphere at 37 °C, the cells were seeded at a density of 1×10^4 cells/well into 96-well plates in complete medium. In the following day, cells at 60-80% confluency were treated with doses between 35-350 and 4.9-49 μg/mL for the degradation products of MB loaded hydrogels based on PEGDA (H1) and HDDA (H2), respectively, and incubated for 24 more hours in a 5% CO_2 incubator at 37 °C. Viability of the cells was evaluated with the MTT assay. According to the manufacturer's protocol, the medium in each well was replenished with 100 μL fresh medium

containing 10 µL of MTT solution (5 mg/mL in PBS) and incubated for 3 h at 37 °C in 5% CO_2. Then, the formed purple formazan crystals were dissolved using 100 µL DMSO solution. Absorbance from each well was determined by a microplate reader (BioTek ELx800 Absorbance Microplate Reader) at 570 nm. Untreated cells were considered as control cells with 100% viability. Each experiment was done in six replicas. Cell viability was calculated according to the equation

$$Cell\ viability\ (\%) = \left[\frac{sample\ absorbance}{control\ absorbance}\right] x\ 100 \quad (5)$$

For the PDT studies, cells cultured and treated as described above were treated with degradation products of MB containing H1 and H2 hydrogels. After 24 h incubation, the medium was replaced with fresh culture medium to remove un-internalized degradation products and/or MB. A laser beam (635 nm wavelength, 300 mW/cm^2 power density, 0.5 cm beam diameter, 30 J/cm^2 energy density) was applied for 100 seconds to the experiment groups. 16 µM free MB was applied as a control, since it corresponds to the highest concentration of MB in release solutions of H1 and H2. The impact of laser treatment on cells which lack the degradation products or MB was also determined. Untreated cells were used as controls. Cell viability was determined before and after laser treatment by MTT assay where cells were incubated at 37 °C for 3 h in 100 µl MTT/DMEM (1:10) solution followed by solubilization of formazan with 100 µl of DMSO and absorbance reading at 570 nm wavelength.

Cytotoxicity was tested also on MCF-7 human breast cancer cell line to confirm cytocompatibility using the same procedure.

Statistical Analysis

Statistical analyses of the degradation products were assessed by using one-way ANOVA analysis followed by Tukey's b comparison test in SPSS. The data were presented as mean ± standard deviation (SD) (n=6). $p < 0.05$ was accepted as statistically significant.

RESULTS & DISCUSSION

One-Step Synthesis and Characterization of PBAE Hydrogels

PBAE hydrogels were prepared in one step by mixing a diacrylate or a diacrylate mixture with a primary diamine to form the hydrogels by an aza-Michael reaction (Figure 1). Different synthetic procedures for aza-Michael addition reactions have been reported before which mostly require elevated temperatures or catalysts such as transition metal and lanthanide halides, triflates, silica gel, heterogeneous solid salts, ionic liquids or boric acid [47-52]. Here, we used a simple and green approach by conducting the reactions in water at 37 °C without any catalyst [53]. These mild conditions also resulted in high yields within a shorter period of time (15-40 min) when compared to other methods which require catalysts (2-8 h) (Table 1). The presence of water facilitates the reaction by activating both the amine and the acrylate through hydrogen bonding. Since the precursor solution is liquid, it is also possible to inject the mixture and obtain the gel *in situ* [19]. This possibility coupled with the occurrence of gelation at physiological conditions provides the potential of easy administration into the human body and hence great practicality.

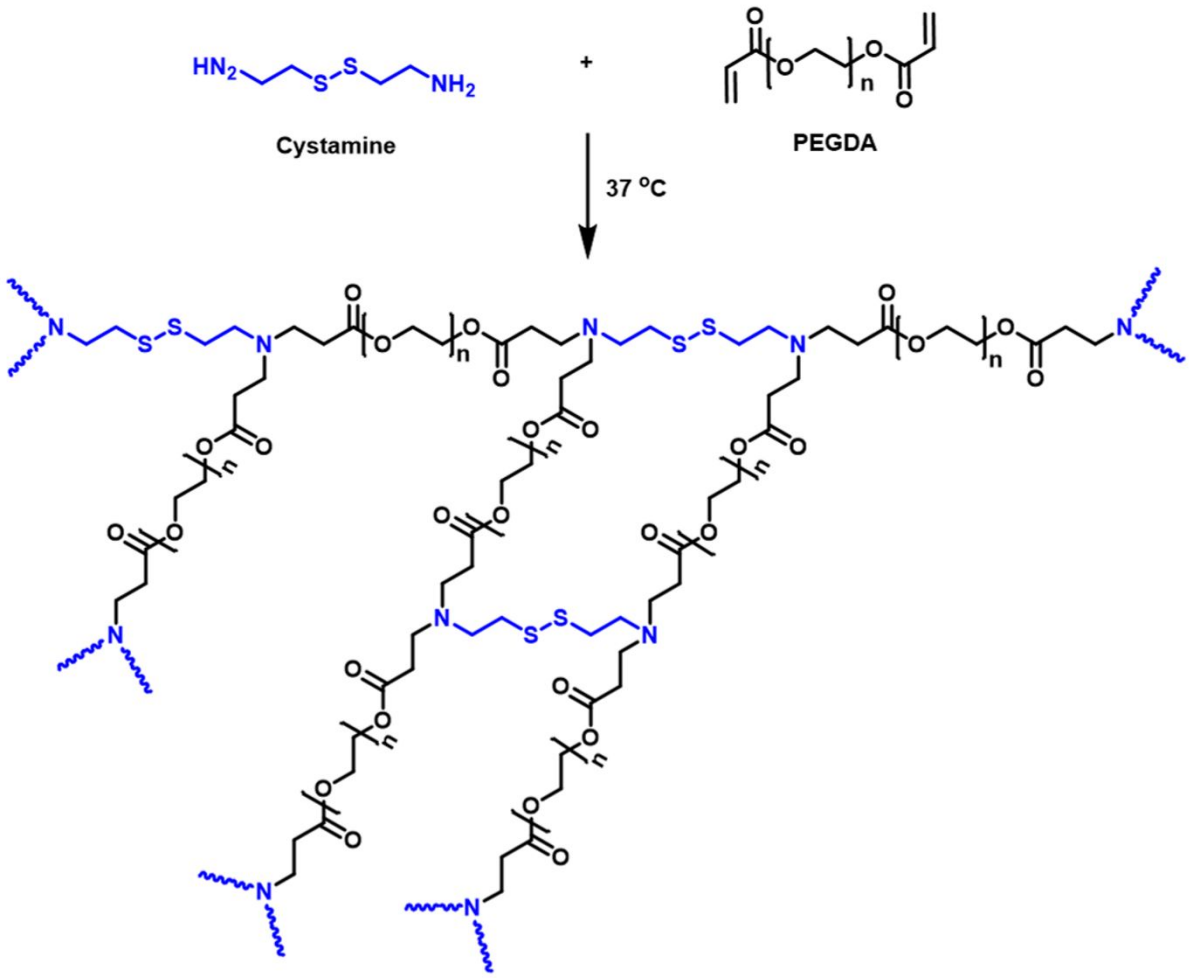

Figure 1. One-step synthesis of H1 from the aza-Michael reaction of PEGDA and cystamine.

The choice of diacrylate and diamine, and their relative ratio determines the physical properties of the hydrogels. Herein we selected PEGDA alone and together with HDDA at different molar ratios to tune the hydrophilicity and accordingly the degradability of the hydrogels. Cystamine was used as the primary diamine due to the redox responsive disulfide bond in its molecular structure. The disulfide group is known to be stable in blood but cleaves rapidly by glutathione in the intracellular environment [28]. Hence, the incorporation of disulfide groups into the hydrogels would render them responsive to the reducing environment.

Three hydrogels with different hydrophilicities were thus synthesized: The H1 hydrogel was solely produced from PEGDA, while the H2 and H3 hydrogels were made from a 1:1 and 1:3 mol ratios of PEGDA and HDDA to reduce the hydrophilic nature (Table 1). We intended to synthesize a fourth hydrogel, H4, from only HDDA but the HDDA/diamine mixture was not soluble in water and no gelation was observed. Both hydrogels H1 and H2 were obtained with high gelation percentages, 95% and 92% respectively, whereas H3 resulted in slightly lower gelation percentage probably due to poor solubility of the HDDA-rich mixture in water.

Table 1. Properties of hydrogels.

Hydrogel	PEGDA:HDDA Mole ratio	Gelation (%)	T_g (°C)
H1	1:0	95	-46
H2	1:1	92	-40
H3	1:3	78	-
H4	0:1	No gelation	-

We monitored gelation reactions between cystamine and the diacrylates PEGDA and HDDA by real-time dynamic rheological measurements in order to follow formation of PBAE hydrogel networks. Figures 2a and 2b show the storage modulus *G'* (filled symbols), loss modulus *G''* (open symbols), and the loss factor *tan δ* (= *G''/ G'*, lines in b) of H1, H2 and H3 reaction solutions at an angular frequency ω of 6.3 rad/s and at a strain amplitude γ_o of 1% as a function of the reaction time. The inset in (a) shows the same *G'* vs time data in a semi-logarithmic scale up to 80 min. It is seen that the initial reaction period during which the dynamic moduli remain unchanged, that is, the induction period, varies depending on the composition of the diacrylate mixture. The H1

gelation solution containing PEGDA only exhibits an induction period of 27 ± 5 min, whereas it shortens to 6 ± 2 min and under 1 min in H2 and H3 solutions with PEGDA mole ratios of 1:1 and 1:3, respectively. Thus, the presence of the more hydrophobic HDDA significantly decreases the induction period of the polymerization reactions. This can be explained by the hydrophobic interactions between HDDA segments leading to the formation of temporary cross-links in the gelation solution [54, 55]. Following the induction period, a crossover between *G'* and *G''* occurs after 35±4, 12±2 and 23±5 min for H1, H2 and H3 hydrogel systems, respectively, which corresponds to the onset of gelation. Eliminating the induction period, this indicates the onset of gelation within 10-20 min for reaction systems. After gelation, *G'* rapidly increases and *tan δ* decreases until they approach plateau values after about 60 min. The tests could not be conducted for longer times due to the appearance of some scatter in the dynamic moduli data. Therefore, the limiting moduli G'_{∞} of the hydrogels were estimated by fitting the experimental *G'* vs reaction time t data to the modified Hill equation [56-58].

$$G'(t) = G'_{\infty}\frac{t^n}{t^n + \theta^n} \tag{6}$$

where θ and n are constants. The solid curves in Fig.2a are the best fits of Eq. (6) to the experimental data indicating that Eq. 6 well simulates the gelation process of the solutions. The limiting values of *G'* obtained from the fits are 35, 56 and 104 kPa for H1, H2 and H3 respectively. Figure 2c shows *G'* (filled symbols) and *G''* (open symbols) of H2 and H3 hydrogels at 37 °C plotted against the frequency ω. *G'* is 59±2 and 78±4 kPa for H2 and H3, respectively, and independent on the frequency ω while *G''* is around 2 orders of magnitude smaller than *G'*, which

is typical behavior of strong gels with a chemically cross-linked network structure. Because *G'* of such hydrogels corresponds to the equilibrium shear modulus *G*, one may estimate their effective cross-link densities ν_e by [59,60]

$$G = 0.5 \nu_e RT \quad (7)$$

where *R* is the gas constant and *T* is the absolute temperature. Eq. 7 assumes a phantom network behavior and the existence of tetrafunctional cross-links in the hydrogel network. Using Eq. 7 together with limiting values of *G'* at 37 °C, the cross-link density ν_e was calculated as 27, 43, and 81 mol/m^3 for H1, H2, and H3 hydrogels, respectively. The results thus reveal formation of a larger number of effective cross-links after incorporation of hydrophobic HDDA segments into the hydrogel network. An interesting point is a higher loss factor *tan δ* of H2 and H3 as compared to H1, which we attribute to the hydrophobic hexyl segments of HDDA units forming hydrophobic associations and hence creating an energy dissipation mechanism in the gel network [61].

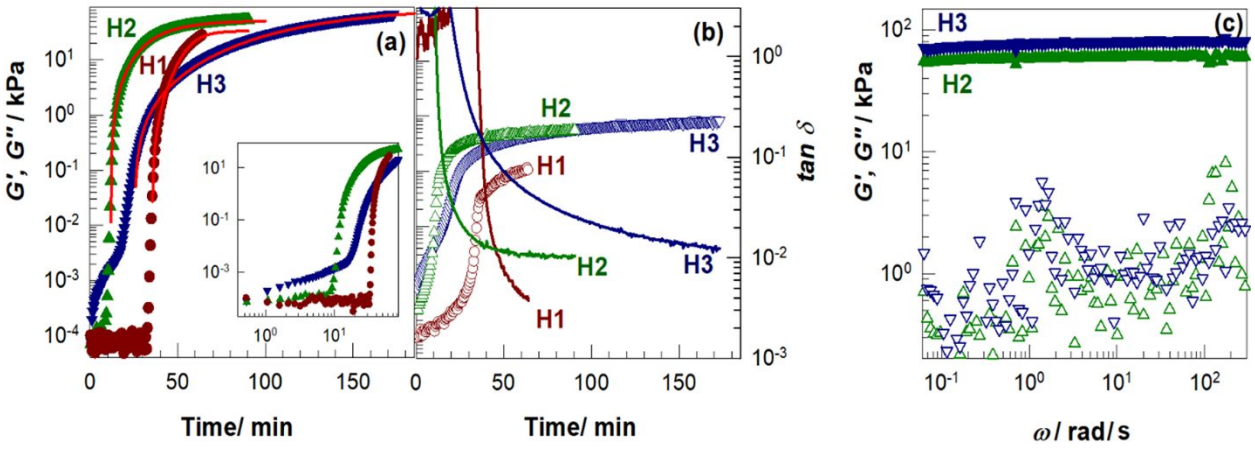

Figure 2. (a, b) Storage modulus *G'* (filled symbols), loss modulus *G''* (open symbols), and *tan* δ (lines in b) as a function of the reaction time. The solid curves in (a) were calculated using Eq. (6). ω = 6.3 rad/s. γ_o = 0.01. Temperature = 37 °C. **(c)** Frequency dependences of *G'* (filled symbols) and *G''* (open symbols) of H2 (triangles up) and H3 hydrogels (triangles down) at 37 °C. γ_o = 0.01.

The thermal properties of the hydrogels were studied using differential scanning calorimetry (DSC). The glass transition temperatures T_g of the hydrogels well correlated with their chemical composition (Table 1). The H2 hydrogel containing HDDA exhibits a higher T_g at -40 °C as compared to H1 with a T_g of -46 °C due to the lower molecular weight. Moreover, the PEGDA based H1 hydrogel shows well-defined narrow transition peaks whereas incorporation of HDDA into the network leads to broader peaks which imply heterogeneity within the system (Figure 3a). The presence of the disulfide group in the hydrogel structure was verified by Raman spectroscopy from the ν_{SS} and ν_{CS} bands observed at 504 and 647 cm^{-1} for H1, 508 and 644 cm^{-1} for H2, and 509 and 644 cm^{-1} for H3, respectively (Figure 3b).

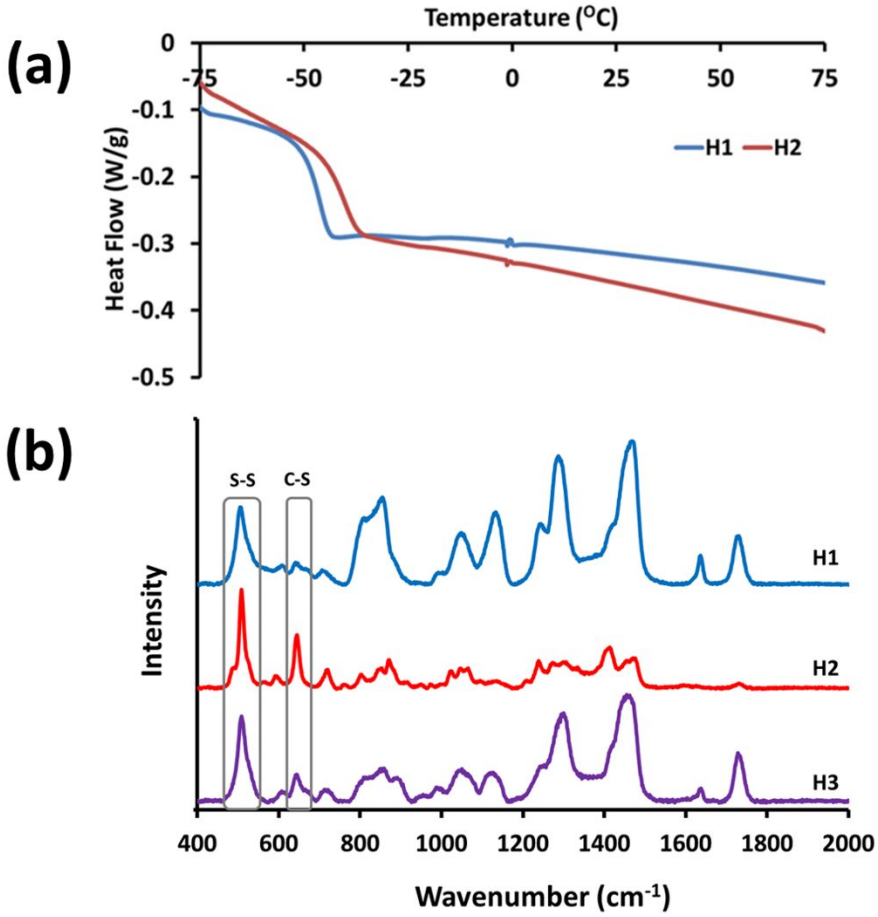

Figure 3. (a) DSC profiles of the H1 and H2 hydrogels under nitrogen at a scanning rate of 10 °C/min, (b) Raman spectra of one-step PBAE hydrogels.

Swelling and Degradation Studies

The effects of the chemical composition of the hydrogels and the pH of the medium on the swelling and degradation kinetics were evaluated, the swelling studies being conducted for up to 3 hours, since the H1 hydrogel started to degrade due to the hydrolysis of β-aminoesters on the backbone. Figures 4a, b show time-dependent swelling and degradation profiles, respectively, of H1, H2 and H3 hydrogels at pH = 5.0 and 7.4.

It was observed that H1 swells approximately two-fold when compared to H2 after a swelling time of 3 h, the swelling increasing only slightly from pH 7.4 to pH 5; while the swelling of H3 at pH 7.4 is lower, like H2, and at pH 5 higher, like H1. The degradation rate of H1 is high, reaching complete degradation within 24 h in both buffers; the rate of H2 is lower and pH-dependent, completely degrading in 120 h in the pH 5 buffer, and 144 h in pH 7.4 buffer (15% and 25% at pH 7.4 and pH 5 in 24 h); and the rate of H3 is lowest and also pH-dependent, degrading only by 28% and 55% after 10 days at pH 7.4 and pH 5, respectively (less than 5% at both pH values in 24 h).

The higher swelling of H1 compared to H2 can be explained as due to the presence of hydrophilic PEGDA units and the lower crosslink density of H1 hydrogels. The swelling of H3 is comparable to either H1 or H2, depending on the pH, despite the high crosslink density and the higher ratio of the hydrophobic HDDA; which might be explained by the possibly heterogeneous structure of H3, forming microscopic hydrophilic regions that absorb water.

The higher swelling of hydrogels in pH 5 buffer compared to those in pH 7.4 probably occurs due to partial protonation of amine groups under acidic conditions creating an electrostatic repulsion of ions expanding the gel network. This effect seems weak for H1 and H2, but strong for H3, possibly due to easier protonation of the amines in the hydrophilic regions hypothesized above.

When the hydrogels are swollen, there is a larger amount of water in the hydrogel structure; so the degradation behavior is expected to be correlated with the hydrogel's swelling, in addition to the overall hydrophilicity. Hence, the pH of the swelling/degradation medium had a limited effect on degradation kinetics for H1 and H2; whereas it had a significant effect in case of H3 where the degradation also was almost two-fold at pH 5 compared to that of at pH 7.4. (Figure 4b). As for the effect of the hydrogels' hydrophilic/hydrophobic character, the degradation can be seen to proceed faster for the more hydrophilic ones, as can be seen from the data reported above, and

Figure 4b. These studies show that it is possible to tune the degradation rate of these one-step hydrogels by manipulating the hydrophilic/hydrophobic balance by selection of starting materials.

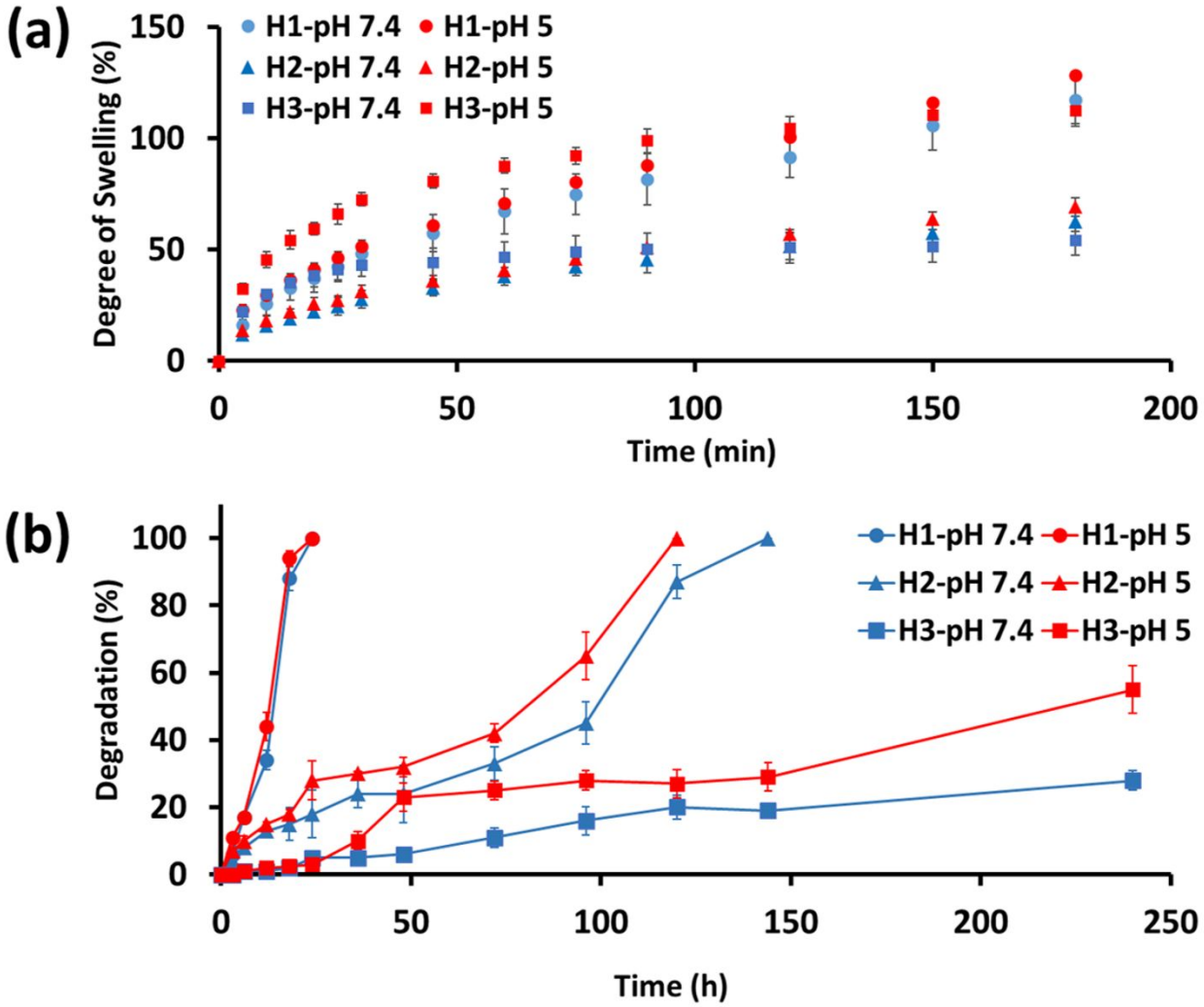

Figure 4. (a) pH dependent swelling profile of one-step PBAE hydrogels at pH 5 and pH 7.4, (b) pH dependent degradation profile of one-step PBAE hydrogels at pH 5 and pH 7.4. (Dry hydrogel thickness is 3 mm and dry hydrogel diameter is 8 mm)

Redox Response

In order to show the redox response, hydrogels were incubated in PBS (pH 7.4) containing 25 mM DTT at 37 °C. Hydrogels were also immersed in pure PBS as a control. Hydrogels exposed to DTT degraded under the reducing conditions via cleavage of disulfide bonds. The visual images and the mass loss of the hydrogels were recorded as a function of time during the degradation period (Figure 5). When either just PBS or PBS+DTT solutions were used, H3 showed slowest degradation profiles followed by H2 due to the hydrophobic nature of HDDA in their structure. As H2 and H3 degraded, HDDA containing insoluble linear polymer fragments were released into the solution causing turbidity. By the end of 12 h, H1 and H2 completely degraded in DTT, whereas H3 degraded 52%. In the same time interval the hydrogels in PBS degraded 34%, 13% and 2% for H1, H2 and H3, respectively, clearly showing the effect of the redox-state on degradation.

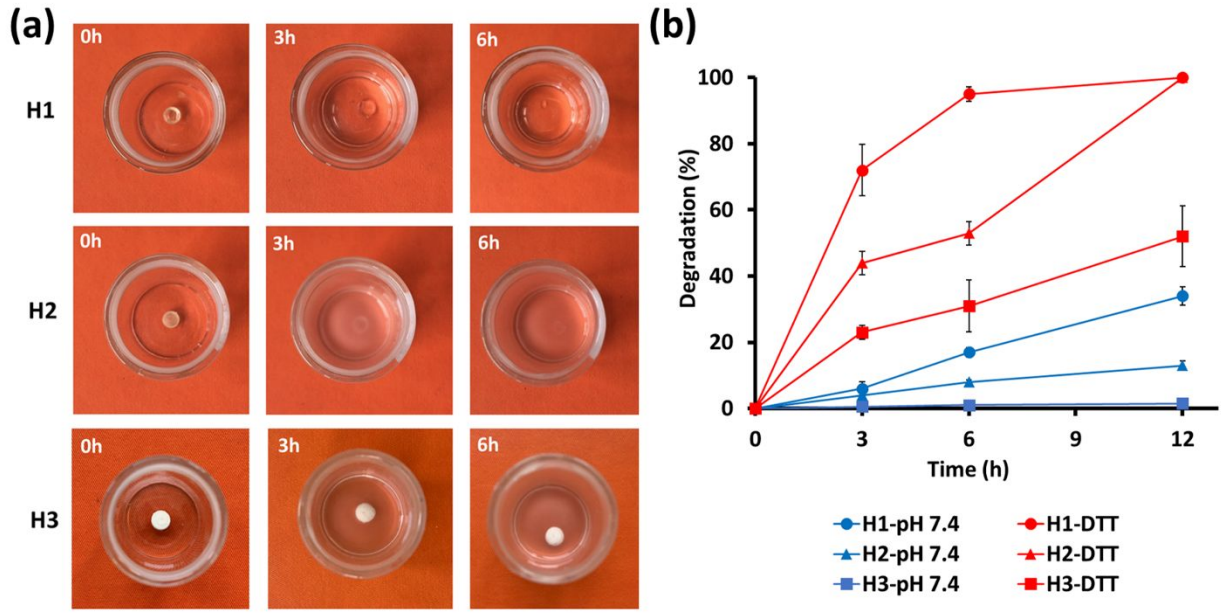

Figure 5. (a) Visual images of H1, H2 and H3 at the beginning and after 3 h and 6 h incubation in DTT at 37 °C. (b) Redox dependent degradation profiles of H1, H2 and H3 in PBS or DTT at 37 °C.

The effect of redox-triggered degradation via exposure to DTT on the morphology of H1, H2 and H3 was evaluated from the SEM images (Figure 6). The initial morphologies of H1 and H2 are very similar, and exhibit a smooth rubber-like and non-porous structure (Figure 6a and 6c) whereas H3 shows an irregular fracture surface (Figure 6e). After degradation, the H1 surface becomes somewhat less smooth (Figure 6c), whereas irregular pores and trenches appear in the H2 fracture surface (Figure 6d). The H3 surface (Figure 6f), on the other hand, develops even more irregular structure, with pores of various sizes. This difference in degradation characteristics can be explained by degradation of hydrophilic PEGDA-containing segments into water soluble polymer chains leaving voids between the hydrophobic-HDDA containing segments.

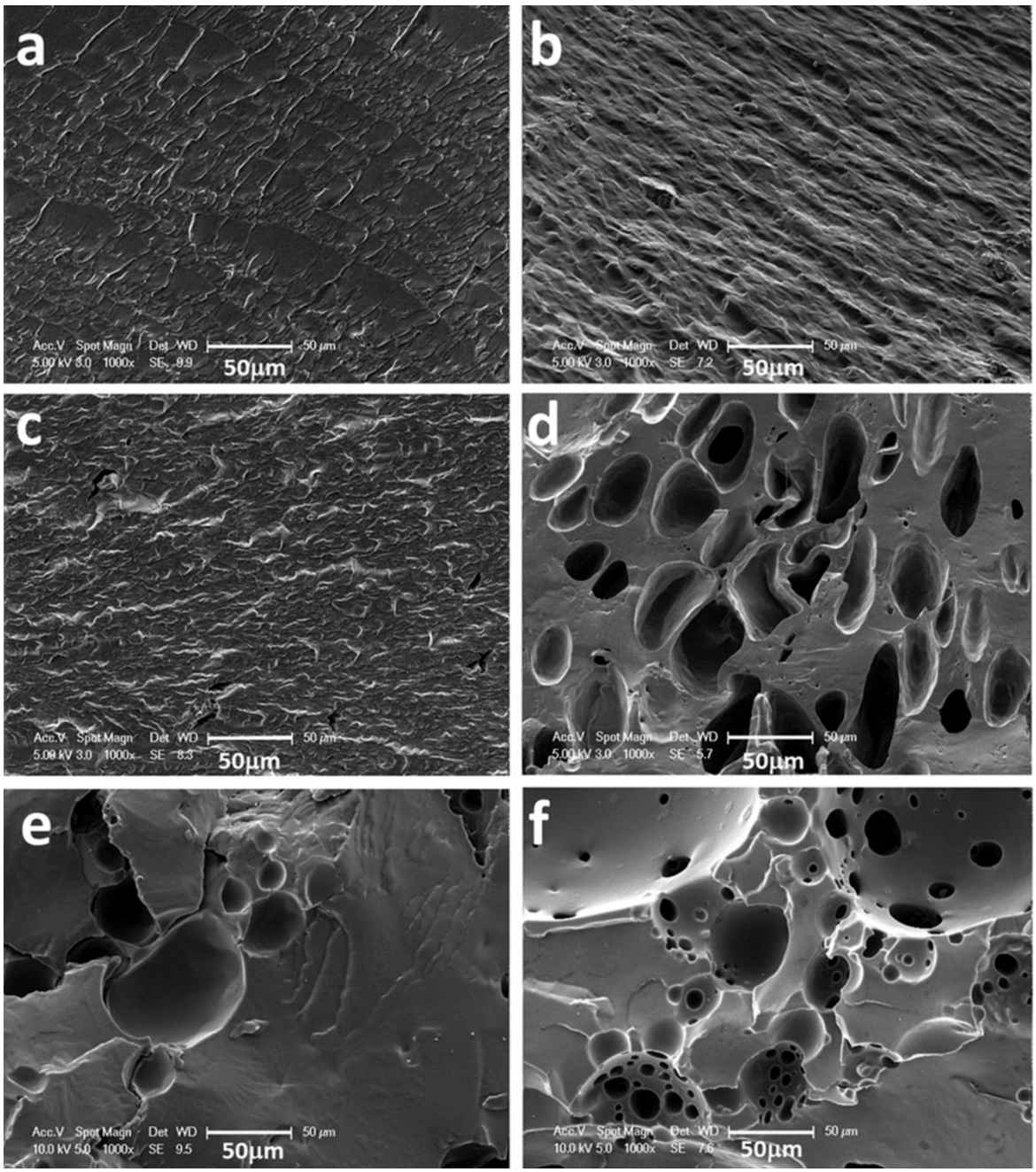

Figure 6. SEM images of hydrogels before and after redox-triggered degradation. a) H1 before degradation, b) H1 after 6 h degradation, c) H2 before degradation, d) H2 after 6 h degradation, d) H3 before degradation, e) H3 after 6 h degradation (Scale bar represents 50 µm).

Drug Loading and *in vitro* Release Studies

MB was selected as a model drug and photosensitizer for photodynamic therapy (PDT) and, it was loaded into the hydrogels during their synthesis process. MB was loaded by 1% wt into the hydrogels and the loading capacity was found to be 0.40±0.03 % for H1 and 0.46±0.04 % for H2 respectively. The effect of the chemical composition, thus hydrophobic/hydrophilic nature of the hydrogels on the release behavior of MB was investigated by UV-visible spectroscopy. The release studies were performed in pH 7.4 and pH 5 buffer solutions to observe the effect of pH on the release profile of the cargo molecule (Figure 7). For H1, release of MB is slightly faster at pH 5 than pH 7.4 until 24 h where the cumulative release at each pH becomes equal. Soon after 24 h, both hydrogels release all of their content due to total degradation of the network structure. No significant effect of pH on the release of MB from H2 was observed. At 24 h the cumulative release of MB is approximately 80% from H2 hydrogels in either pH. Considering the slow degradation of H2, we assume that most of MB is released by diffusion due to expansion of hydrogel dimensions as the hydrogel swells. The rest of the MB was probably entrapped in the more hydrophobic domains left behind after the initial degradation of the PEGDA rich regions of H2. Therefore, much slower release of MB was observed after the first 24 h and full release was obtained only after full degradation after 120 h.

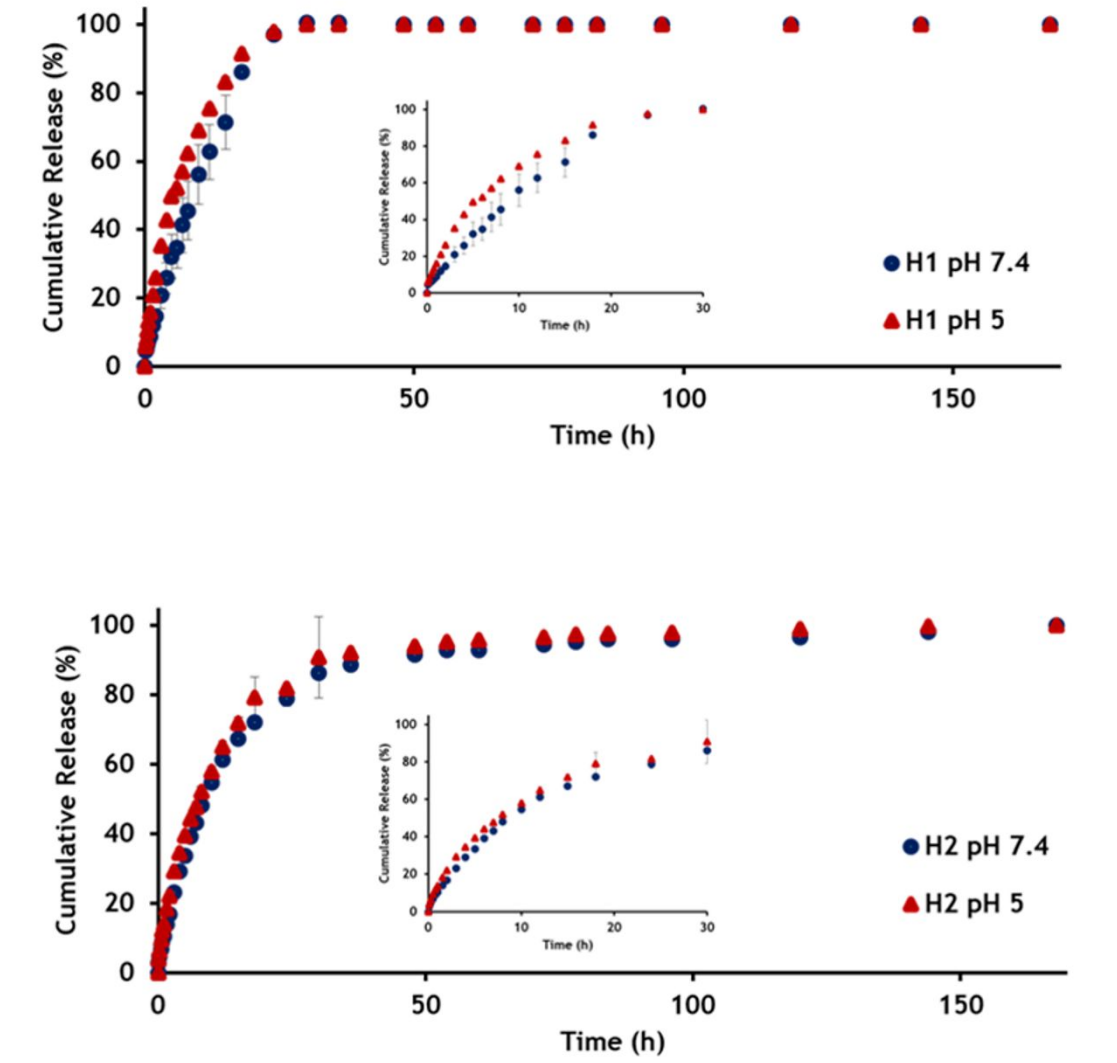

Figure 7. pH-dependent release kinetics of MB from H1 and H2 at 37 °C and two different pH values (insets: the first 30 h, also given in SI)

In Vitro Cytotoxicity and Photodynamic Therapy

The degradability of the hydrogels both via hydrolysis and by cleavage of disulfide bonds, into non-toxic degradation products can eliminate the need for later surgical removal from the human body, both for tissue scaffold and drug/gene delivery applications. The dose dependent cytotoxicity of degradation products of PBAE hydrogels (after 24 h degradation) in PBS (pH 7.4)

was assessed on MCF-7 cells after 24 h incubation (Figure 8). Viability of cells was above 80% at all doses which indicates that degradation products are non-cytotoxic in the range of 1-200 µg/mL in MCF-7 cells according to the ISO 10993–5 classification [62]. Overall, looking at the whole concentration range, degradation products of all tested compositions look safe with no dramatic difference between them.

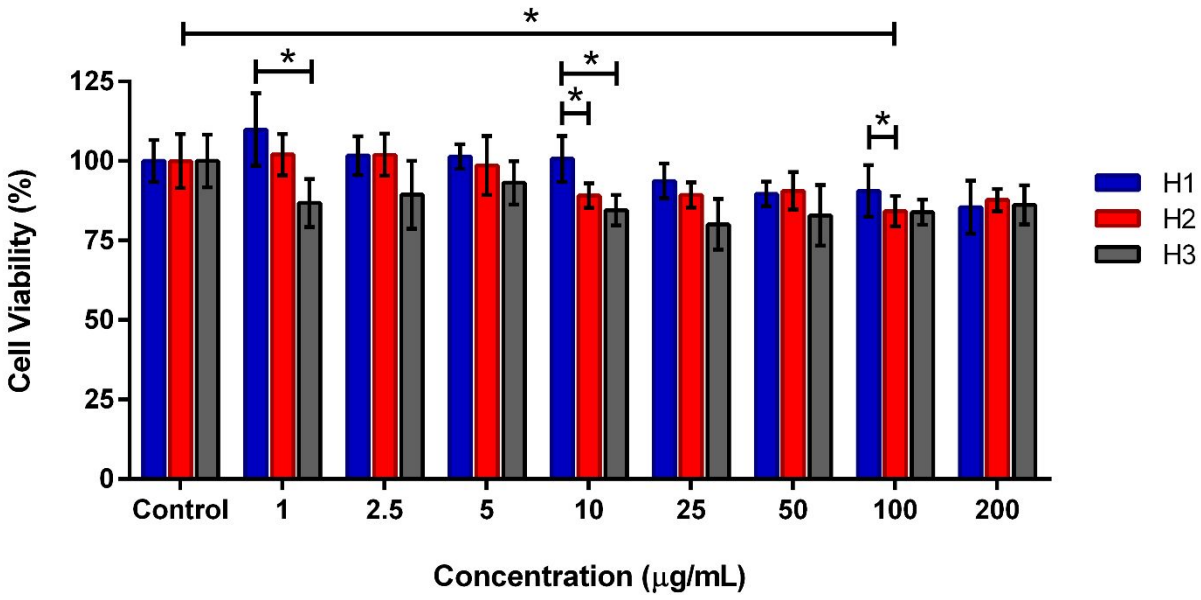

Figure 8. The effect of degradation products of the hydrogels on cell viability of MCF-7 human breast cancer cells. Cells were treated with different concentrations of the degradation products for 24 h. Untreated cells were used as the control. The cell viability test was performed by MTT assay (±SD; $n = 5$; $p < 0.05$ (*) compared with all concentrations).

To understand whether the released MB retained its biological activity or not, and to demonstrate local drug delivery potential of these PBAE hydrogels, *in vitro* PDT study was performed with the degradation products of the hydrogels (Figure 9). MB loaded H1 and H2 were degraded for 6 h in PBS and then both dark toxicity, impact of laser irradiation on the viability of untreated cells and

the influence of PDT on cell viability were tested in a dose dependent manner using A549 cell lines. For this part, a lung cancer cell line was preferred because the lung is an appropriate target organ for phototherapies which can be performed via endoscopic methods [44, 63]. Free MB (16 μM) was also applied to cells at the highest concentration of MB in H1 and H2 degradation products. A549 cells were incubated with degradation products of MB loaded H1 and H2 in a dose range of 35-350 μg/ml, and 4.9-49 μg/mL, respectively, for 24 h. The difference in the dose range originates from the different degradation rates of H1 and H2 hydrogels. After the medium is replenished, each experiment's groups were treated for 100 seconds with a laser light of 30 J/cm^2 energy density at 635 nm. As seen in Figure 9b, the control (untreated) and laser control (no degradation product but 100 sec laser irradiation) groups showed no decrease in viability. However, cells incubated with MB containing degradation products and treated with laser showed a tremendous drop in cell viability due to cytotoxic effect of photodynamic therapy well established in the literature [42-44, 63]. This indicates that there is no significant dark toxicity of MB loaded hydrogels and the laser irradiation does not reduce viability of cells if there is no exposure to photosensitizer, as desired. In addition, the toxicity of released MB was similar to free MB (16 μM), implying that encapsulation and release of MB by one-step PBAE hydrogels did not hamper its function as a photosensitizer and it retained biological activity. Elaborate experiments showing the cell death mechanism is beyond the scope of this study, but the effect is well established as indicated by the references.

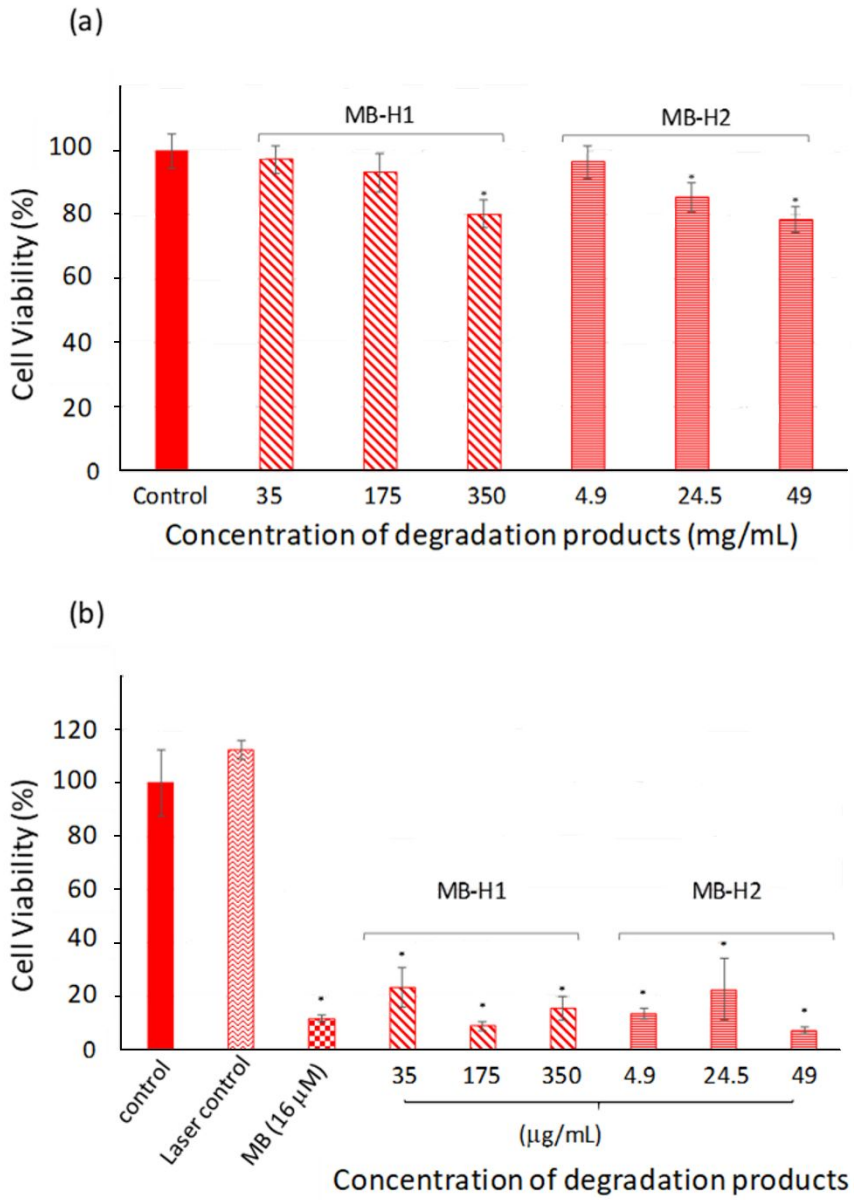

Figure 9. (a) The effect of released MB and degradation products on viability of A549 cells after 24 h exposure. Untreated cells were used as a control. (b) The effect of released MB and degradation products on cell viability of A549 cells after laser treatment (635 nm, 100 s, 30 J/cm^2). Untreated cells were used as a control. Cells were not treated with MB-hydrogel degradation products but subjected to laser irradiation were used as the laser control. (±SD; $n = 6$; $p < 0.05$ (*) compared with all concentrations).

CONCLUSIONS

A simple one-step synthesis strategy based on aza-Michael reaction with no byproducts was used to prepare novel PBAE hydrogels. By selecting the building blocks the hydrophilicity/hydrophobicity and accordingly the swelling and degradation behavior of the hydrogels were tailored. The hydrogels were loaded with MB as a model drug by simply adding the drug molecule into the precursor mixture. The hydrogels showed response to external triggers such as pH and redox state which served as a tool to facilitate the on-demand degradation of the hydrogel into nontoxic materials and release of the cargo molecule in a controlled manner. The biological activity of the released MB was evaluated by photodynamic therapy. Overall, these systems have the potential to be used as platforms for controlled delivery of therapeutic agents.

ASSOCIATED CONTENT

Supporting Information.

Storage modulus *G'* (filled symbols) and loss modulus *G''* (open symbols) of H2 hydrogel plotted against the strain amplitude γ_o at ω = 6.3 rad/s. Temperature 37 °C; pH-dependent release kinetics of MB from H1 and H2 at 37 °C and two different pH values

AUTHOR INFORMATION

Corresponding Author

* avcid@boun.edu.tr

Present Addresses

[#] WestCHEM School of Chemistry, University of Glasgow, G12 8QQ, Glasgow, United Kingdom.

[§]Department of Biomedical Engineering, Erzincan Binali Yildirim University, 24100 Erzincan, Turkey.

[‖]Department of Chemistry and Chemical Processing Technologies, Kirklareli University, Luleburgaz, 39750 Kirklareli, Turkey.

Author Contributions

The manuscript was written through contributions of all authors. All authors have given approval to the final version of the manuscript.

Funding Sources

This study was supported by a grant from the Bogazici University Research Fund (Grant no: BAP13842)

ACKNOWLEDGMENT

The authors would like to acknowledge financial support from Bogazici University Research Fund (13842). Betul Bingol thanks the financial support of the Scientific and Technological Research Council of Turkey (TUBITAK) National Scholarship Programme for PhD Students (2211-A).

ABBREVIATIONS

PEGDA, poly(ethylene glycol) diacrylate; HDDA, 1,6-hexanediol diacrylate; PBAE, poly(β-amino ester); MB, methylene blue; PBS, phosphate buffered saline; DTT, 1,4-dithiothreitol; DMEM, Dulbecco's Modified Eagle Medium; FBS, fetal bovine serum; MTT, thiazolyl blue tetrazolium bromide; SEM, scanning electron microscopy; DSC, differential scanning calorimetry.

REFERENCES

[1] Buwalda, S. J.; Boere, K. W. M.; Dijkstra, P. J.; Feijen, J.; Vermonden, T.; Hennink, W. E. Hydrogels in a historical perspective: From simple networks to smart materials. *J. Control. Release* **2014**, *190*, 254–273.

[2] Peppas, N. A.; Hilt, J. Z.; Khademhosseini, A.; Langer, R. Hydrogels in biology and medicine: From molecular principles to bionanotechnology. *Adv. Mater*. **2006**, *18*, 1345–1360.

[3] Hoffman, A. S. Hydrogels for biomedical applications. *Adv. Drug Deliv. Rev.* **2012**, *64*, 18–23.

[4] Lynn D. M.; Langer, R. Degradable Poly(β-amino esters): Synthesis, characterization, and self-assembly with plasmid DNA. *J. Am. Chem. Soc.* **2000***, 122* (44), 10761–10768.

[5] Akyol, E.; Tatliyuz, M.; Demir Duman, F.; Guven, M. N.; Yagci Acar, H.; Avci, D. Phosphonate-functionalized poly(β-amino ester) macromers as potential biomaterials. *J. Biomed. Mater. Res. A* **2018**, *106* (5), 1390–1399.

[6] McBath, R. A.; Shipp, D. A. Swelling and degradation of hydrogels synthesized with degradable poly(β-amino ester) crosslinkers. *Polym. Chem.* **2010**, *1*, 860–865.

[7] Yin, Q.; Shen, J.; Chen, L.; Zhang, Z.; Gu, W.; Li, Y. Overcoming multidrug resistance by co-delivery of Mdr-1 and survivin-targeting RNA with reduction-responsible cationic poly(β-amino esters). *Biomaterials* **2012**, *33*, 6495–6506.

[8] Tamer Y.; Chen, B. Lysine-derived, pH-sensitive and biodegradable poly(beta-aminoester urethane) networks and their local drug delivery behaviour. *Soft Matter* **2018**, *14*, 1195–1209.

[9] Gao, Y.; Huang, J. Y.; Ahern, J. O.; Cutlar, L.; Zhou, D.; Lin, F. H.; Wang, W. Highly branched poly(β-amino esters) for non-viral gene delivery: High transfection efficiency and low toxicity achieved by increasing molecular weight. *Biomacromolecules* **2016**, *17*, 3640–3647.

[10] Newland, B.; Wolff, P.; Zhou, D.; Wang, W.; Zhang, H.; Rosser, A.; Wang, W.; Werner, C. Synthesis of ROS scavenging microspheres from a dopamine containing poly(β-amino ester) for applications for neurodegenerative disorders. *Biomater. Sci.* **2016**, *4* (3), 400–404.

[11] Yu, Y.; Zhang, X.; Qiu, L. The anti-tumor efficacy of curcumin when delivered by size/charge-changing multistage polymeric micelles based on amphiphilic poly(β-amino ester) derivates. *Biomaterials* **2014**, *35* (10), 3467–3479.

[12] Tzeng, S. Y.; Guerrero-Cázares, H.; Martinez, E. E.; Sunshine, J. C.; Quiñones-Hinojosa, A.; Green, J. J. Non-viral gene delivery nanoparticles based on poly(β-amino esters) for treatment of glioblastoma. *Biomaterials* **2011**, *32* (23), 5402–5410.

[13] Cheng, T.; Ma, R.; Zhang, Y.; Ding, Y.; Liu, J.; Ou, H.; An, Y.; Liu, J.; Shi, L. A surface-adaptive nanocarrier to prolong circulation time and enhance cellular uptake. *Chem. Commun.* **2015**, *51* (81), 14985–14988.

[14] Liu, Y.; Li, Y.; Keskin, D.; Shi, L. Poly(β-amino esters): Synthesis, formulations, and their biomedical applications. *Adv. Healthcare Mater.* **2019**, *8* (2), 1801359.

[15] Biswal, D.; Wattamwar, P. P.; Dziubla, T. D.; Hilt, J. Z. A single-step polymerization method for poly(β-amino ester) biodegradable hydrogels. *Polymer* **2011**, *52* (26), 5985–5992.

[16] Du, Y.; Yan, H.; Niu, S.; Bai, L.; Chai, F. Facile one-pot synthesis of novel water-soluble fluorescent hyperbranched poly(amino esters). *RSC Adv.* **2016**, *6* (91), 88030–88037.

[17] Wang, J.; Yang, H. Superelastic and pH-responsive degradable dendrimer cryogels prepared by cryo-aza-Michael addition reaction. *Sci. Rep.* **2018**, *8*, 7155.

[18] Lakes, A. L.; Jordan, C. T.; Gupta, P.; Puleo, D. A.; Hilt, J. Z.; Dziubla, T. D. Reducible disulfide poly(beta-amino ester) hydrogels for antioxidant delivery. *Acta Biomater.* **2018**, *68*, 178–189.

[19] Yu L.; Ding, J. Injectable hydrogels as unique biomedical materials. *Chem. Soc. Rev.* **2008**, *37* (8), 1473–1481.

[20] Li, Y.; Rodrigues, J.; Tomás, H. Injectable and biodegradable hydrogels: Gelation, biodegradation and biomedical applications. *Chem. Soc. Rev.* **2012**, *41* (6), 2193–2221.

[21] Xu, Q.; Guo, L.; A, S.; Gao, Y.; Zhou, D.; Greiser, U.; Creagh-Flynn, J.; Zhang, H.; Dong, Y.; Cutlar, L.; Wang, F.; Liu, W.; Wang, W.; Wang, W. Injectable hyperbranched poly(β-amino ester) hydrogels with on-demand degradation profiles to match wound healing processes. *Chem. Sci*. **2018**, *9* (8), 2179–2187.

[22] Xu, Q.; Venet, M.; Wang, W.; Creagh-Flynn, J.; Wang, X.; Li, X.; Gao, Y.; Zhou, D.; Zeng, M.; Lara-Sáez, I.; A, S.; Tai, H.; Wang, W. Versatile hyperbranched poly(β-hydrazide ester) macromers as injectable antioxidative hydrogels. *ACS Appl. Mater. Interfaces* **2018**, *10* (46), 39494−39504.

[23] Guk, K.; Lim, H.; Kim, B.; Hong, M.; Khang, G.; Lee, D. Acid-cleavable ketal containing poly(β-amino ester) for enhanced siRNA delivery. *Int. Journal Pharm.* **2013**, *453* (2), 541–550.

[24] Deng, X.; Zheng, N.; Song, Z.; Yin, L.; Cheng, J. Trigger-responsive, fast-degradable poly(β-amino ester)s for enhanced DNA unpackaging and reduced toxicity. *Biomaterials* **2014**, *35* (18), 5006–5015.

[25] Liu, S.; Gao, Y.; A, S.; Zhou, D.; Greiser, U.; Guo, T.; Guo, R.; Wang, W. Biodegradable highly branched poly(β-amino ester)s for targeted cancer cell gene transfection. *ACS Biomater. Sci. Eng.* **2017**, *3* (7), 1283–1286.

[26] Zhang, Y.; Wang, R.; Hua, Y.; Baumgartner, R.; Cheng, J. Trigger-responsive poly(β-amino ester) hydrogels. *ACS Macro Lett.* **2014**, *3* (7), 693–697.

[27] Meng, F.; Hennink, W. E.; Zhong, Z. Reduction-sensitive polymers and bioconjugates for biomedical applications. *Biomaterials* **2009**, *30* (12), 2180–2198.

[28] Huo, M.; Yuan, J.; Tao, L.; Wei, Y. Redox-responsive polymers for drug delivery: from molecular design to applications. *Polym. Chem.* **2014**, *5* (5), 1519–1528.

[29] Robertson, C. A.; Hawkins Evans, D.; Abrahamse, H. Photodynamic therapy (PDT): A short review on cellular mechanisms and cancer research applications for PDT. *J. Photochem. Photobiol. B Biol*. **2009**, *96* (1), 1–8.

[30] Ormond, A. B.; Freeman, H. S. Dye sensitizers for photodynamic therapy. *Materials* **2013**, *6* (3), 817–840.

[31] Castano, A. P.; Demidova, T. N.; Hamblin, M. R. Mechanisms in photodynamic therapy: Part one - photosensitizers, photochemistry and cellular localization. *Photodiagnosis Photodyn. Ther.* **2004**, *1* (4), 279–293.

[32] Zhang, X.; Xia, L. Y.; Chen, X.; Chen, Z.; Wu, F. G. Hydrogel-based phototherapy for fighting cancer and bacterial infection. *Sci. China Mater.* **2017**, *60* (6), 487–503.

[33] Donnelly, R. F.; Morrow, D. I. J.; McCrudden, M. T. C.; Alkilani, A. Z.; Vicente-Pérez, E. M.; O'Mahony, C.; González-Vázquez, P.; McCarron, P. A.; Woolfson, A. D. Hydrogel-forming and dissolving microneedles for enhanced delivery of photosensitizers and precursors. *Photochem. Photobiol.* **2014**, *90* (3), 641–647.

[34] Fraix, A.; Gref, R.; Sortino, S. A multi-photoresponsive supramolecular hydrogel with dual-color fluorescence and dual-modal photodynamic action. *J. Mater. Chem. B* **2014**, *2* (22), 3443–3449.

[35] Wang, Y.; Han, B.; Shi, R.; Pan, L.; Zhang, H.; Shen, Y.; Li, C.; Huang, F.; Xie, A. Preparation and characterization of a novel hybrid hydrogel shell for localized photodynamic therapy. *J. Mater. Chem. B* **2013**, *1* (46), 6411–6417.

[36] Zhang, H.; Shi, R.; Xie, A.; Li, J.; Chen, L.; Chen, P.; Li, S.; Huang, F.; Shen, Y. Novel TiO_2/PEGDA hybrid hydrogel prepared in situ on tumor cells for effective photodynamic therapy. *ACS Appl. Mater. Interfaces* **2013**, *5* (23), 12317–12322.

[37] Donnelly, R. F.; Cassidy, C. M.; Loughlin, R. G.; Brown, A.; Tunney, M. M.; Jenkins, M. G.; McCarron, P. A. Delivery of methylene blue and meso-tetra (N-methyl-4-pyridyl) porphine tetra tosylate from cross-linked poly(vinyl alcohol) hydrogels: A potential means of photodynamic therapy of infected wounds. *J. Photochem. Photobiol. B Biol.* **2009**, *96* (3), 223–231.

[38] Fallows, S. J.; Garland, M. J.; Cassidy, C. M.; Tunney, M. M.; Singh, T. R. R.; Donnelly, R. F. Electrically-responsive anti-adherent hydrogels for photodynamic antimicrobial chemotherapy. *J. Photochem. Photobiol. B Biol.* **2012**, *114*, 61–72.

[39] Parsons, C.; McCoy, C. P.; Gorman, S. P.; Jones, D. S.; Bell, S. E. J.; Brady, C.; McGlinchey, S. M. Anti-infective photodynamic biomaterials for the prevention of intraocular lens-associated infectious endophthalmitis. *Biomaterials* **2009**, *30* (4), 597–602.

[40] Chen, C. P.; Hsieh, C. M.; Tsai, T.; Yang, J. C.; Chen, C. T. Optimization and evaluation of a chitosan/hydroxypropyl methylcellulose hydrogel containing toluidine blue O for antimicrobial photodynamic inactivation. *Int. J. Mol. Sci.* **2015**, *16* (9), 20859–20872.

[41] Spagnul, C.; Greenman, J.; Wainwright, M.; Kamil, Z.; Boyle, R. W. Synthesis, characterization and biological evaluation of a new photoactive hydrogel against Gram-positive and Gram-negative bacteria. *J. Mater. Chem. B* **2016**, *4* (8), 1499–1509.

[42] dos Santos, A. F.; Terra, L. F.; Wailemann, R. A. M.; Oliveira, T. C.; Gomes, V. M.; Mineiro, M. F.; Meotti, F. C.; Bruni-Cardoso A.; Baptista, M. S.; Labriola, L. Methylene blue photodynamic therapy induces selective and massive cell death in human breast cancer cells. *BMC Cancer* **2017**, *17* (1), 1–15.

[43] Ates, G. B.; Ak, A.; Garipcan, B.; Gulsoy, M. Methylene blue mediated photobiomodulation on human osteoblast cells. *Lasers Med. Sci.* **2017**, *32* (8), 1847–1855.

[44] Lim, E. J.; Oak, C. H.; Heo, J.; Kim Y. H. Methylene blue-mediated photodynamic therapy enhances apoptosis in lung cancer cells. *Oncol. Rep.* **2013**, *30* (2), 856–862.

[45] Koo, H.; Lee, H.; Lee, S.; K. H. Min; Kim, M. S.; Lee, D. S.; Choi, Y.; Kwon, I. C.; Kim, K.; Jeong, S. Y., *In vivo* tumor diagnosis and photodynamic therapy *via* tumoral pH-responsive polymeric micelles. *Chem. Commun*. **2010**, *46*, 5668-5670.

[46] Dispinar, T.; Camp, W. V.; De Cock, L. J.; De Geest, B. G.; Du Prez, F. E. Redox-responsive degradable PEG cryogels as potential cell scaffolds in tissue engineering. *Macromol. Biosci.* **2012**, *12* (3), 383–394.

[47] Reboule, I.; Gil, R.; Collin, J. Aza-Michael reactions catalyzed by samarium diiodide. *Tetrahedron Lett.* **2005**, *46* (45), 7761–7764.

[48] Varala, R.; Alam, M. M.; Adapa, S. R. Chemoselective Michael type addition of aliphatic amines to α,β-ethylenic compounds using bismuth triflate catalyst. *Synlett* **2003**, (5), 720–722.

[49] Basu, B.; Das, P.; Hossain, I. Synthesis of β-amino esters via aza-Michael addition of amines to alkenes promoted on silica: A useful and recyclable surface. *Synlett* **2004**, (14), 2630–2632.

[50] Azizi, N.; Saidi, M. R. $LiClO_4$ accelerated Michael addition of amines to α,β-unsaturated olefins under solvent-free conditions. *Tetrahedron* **2004**, *60* (2), 383–387.

[51] Xu, L.-W.; Li, J.-W.; Zhou, S.-L.; Xia, C.-G. A green, ionic liquid and quaternary ammonium salt-catalyzed aza-Michael reaction of α,β-ethylenic compounds with amines in water. *New J. Chem*. **2004**, *28* (2), 183–184.

[52] Chaudhuri, M. K.; Hussain, S.; Kantam, M. L.; Neelima, B. Boric acid: a novel and safe catalyst for aza-Michael reactions in water. *Tetrahedron Lett.* **2005**, *46* (48), 8329–8331.

[53] Ranu, B. C.; Banerjee, S. Significant rate acceleration of the aza-Michael reaction in water. *Tetrahedron Lett.* **2007**, *48* (1), 141–143.

[54] Tuncaboylu, D.C.; Sarı, M.; Oppermann, W.; Okay, O. Tough and self-healing hydrogels formed via hydrophobic interactions. *Macromolecules* **2011**, *44*, 4997-5005.

[55] Abdurrahmanoglu, S.; Can, V.; Okay, O. Design of high-toughness polyacrylamide hydrogels by hydrophobic modification. *Polymer* **2009**, *50*, 5449-5455.

[56] Calvet, D.; Wong, J. Y.; Giasson, S. Rheological monitoring of polyacrylamide gelation: Importance of cross-link density and temperature. *Macromolecules* **2004**, *37* (20), 7762–7771.

[57] Giraldo, J.; Vivas, N. M.; Vila, E.; Badia, A. Assessing the (a)symmetry of concentration-effect curves. *Pharmacol. Ther.* **2002**, *95* (1), 21–45.

[58] Tavsanli, B.; Okay, O. Mechanically robust and stretchable silk/hyaluronic acid hydrogels. *Carbohydr. Polym.* **2019**, *208*, 413–420.

[59] Flory, P. J. Principles of Polymer Chemistry; Cornell University Press: Ithaca, NY, 1953.

[60] Treloar, L. R. G. The Physics of Rubber Elasticity; Oxford University Press: Oxford, UK, 1975.

[61] Creton, C. 50th Anniversary perspective: Networks and gels: Soft but dynamic and tough. *Macromolecules* **2017**, *50* (21), 8297–8316.

[62] ISO 10993-5:2009 Biological evaluation of medical devices part 5: Tests for in vitro cytotoxicity; ISO: Geneva, Switzerland, 2009.

[63] Obstoy, B.; Salaun, M.; Bohn, P.; Veresezan, L.; Sesboué, R.; Thiberville, L. Photodynamic therapy using methylene blue in lung adenocarcinoma xenograft and hamster cheek pouch induced squamous cell carcinoma. *Photodiagnosis Photodyn. Ther.* **2016**, *15*, 109–114.

SYNOPSIS

For table of contents only.

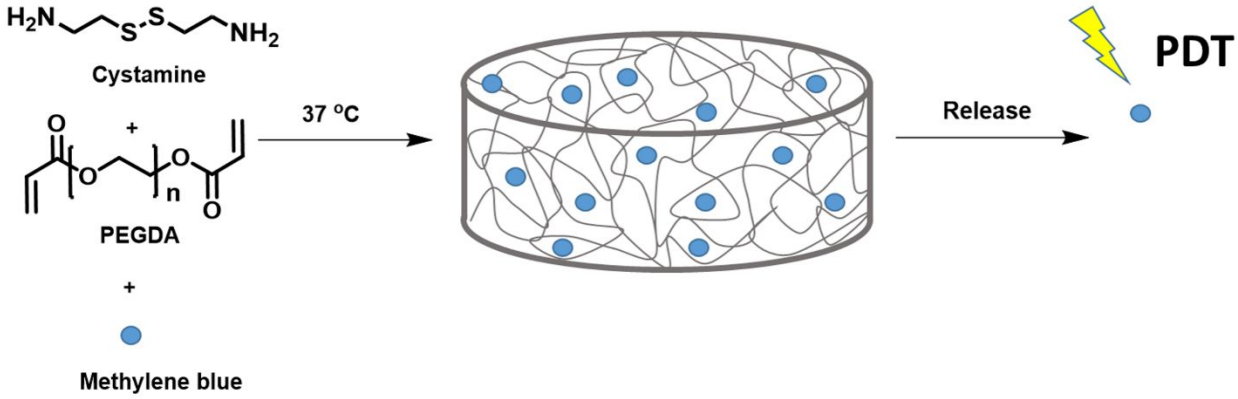

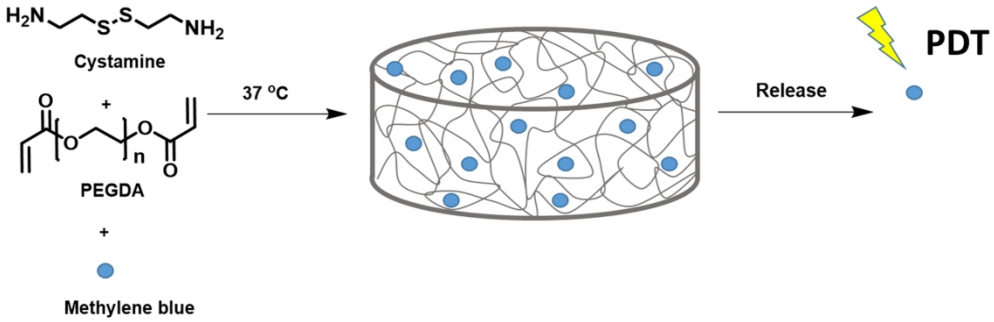

One-step injectable and bioreducible hydrogels for PDT and other biomedical applications

203x76mm (300 x 300 DPI)